EARTH'S CRYOSPHERE
SCIENTIFIC JOURNAL

Earth`s Cryosphere, 2018, vol. XXII, No. 4, pp. 68–74 **http://earthcryosphere.ru/**

METHODS OF CRYOSPHERE RESEARCH

DOI: 10.21782/EC2541-9994-2018-4(68-74)

CHANGES IN PROPERTIES AND STATE OF COAL EXPOSED TO FREEZE-THAW WEATHERING: EVIDENCE FROM THERMALLY INDUCED ACOUSTIC EMISSION

E.A. Novikov, V.L. Shkuratnik, M.G. Zaytsev, R.O. Oshkin

National University of Science and Technology "MISiS", Moscow Mining Institute (MGI), 4, Leninskiy ave., Moscow, 119049, Russia; ftkp@mail.ru, e.novikov@misis.ru

Acoustic emission responses of water-saturated lignite and hard coal samples exposed to cyclic freezing and thawing have been studied as a function of the number of loading cycles, at different stages of freeze-thaw weathering, including prefailure. It is suggested to use an acoustic emission ratio to track the weathering history of coal and to assess the dependence of the weathering rate on pore water pH. The revealed acoustic emission patterns are applicable to predict the effect of weathering on the oxidation of coal which reduces its calorific value and poses risks of spontaneous combustion.

Acoustic emission, fossil coal, freezing, thawing, freeze-thaw weathering, experiment, express testing

INTRODUCTION

Russia has been among the most important holders and producers of coal. However, most of coal deposits reside in the eastern and northern parts of the country, in the zone of perennially or seasonally frozen ground [*Timofeev and Cherepovskiy, 2000–2003; Gresov et al., 2014*]. Periglacial processes in cold regions [*Yershov, 2002; Rogov, 2009*] influence strongly the efficiency and safety of coal mining, especially in the case of open-pit production. Weathering (cracking) caused by diurnal and seasonal temperature changes (cyclic freezing and thawing), as well as percolation of meteoric waters with different pH values, lead to deformation and instability of scraps and slopes in surface coal mines [*Fedorova, 2009; Verkhoturov and Razmakhnina, 2016*]. The cracks become paths for coal aeration [*Yanmei Yu et al., 2012; Shi-Qi Liu et al., 2015*], and the oxygenated air gradually replaces inert pore gases as the cracks grow in size and number. Thus coal exposed in outcrops and open-air stacks experiences rapid aerial oxidation which deteriorates its coking properties, especially the heating value, and poses risks of spontaneous combustion [*Jun Deng et al., 2015*].

The coal structure is commonly studied by examination of sample surfaces under a microscope [*Raja Sen et al., 2009; Qian Zhu, 2014*]. This classical approach is quite well informative but labor consuming; furthermore, it does not allow looking into the sample interior and is inapplicable in the field. There are methods of estimating the current oxidation of coal from its response to special chemical treatment [*ASTM D5263-15, 2015*], but they provide no evidence of pores and cracks and do not allow predictions for further oxidation rates.

Therefore, the existing methods are poorly suitable to study freeze-thaw weathering which is indispensable for maintaining the stability of mining systems, monitoring the state of coalbeds, and preventing avalanche-like oxidation of coal deteriorating its quality.

An alternative approach developed in recent years is to estimate the mechanical stability and thermal resistance of coal using the so-called thermoacoustic emission (TAE). The method stems from the idea that the properties and state of materials are recorded in their acoustic emission responses to thermal shocks [*Shkuratnik et al., 2015*]. Although being still limited, the available TAE data reveal correlation of acoustic emission parameters with the thermal resistance and oxidation degree of coal samples [*Novikov et al., 2013; Shkuratnik and Novikov, 2017*].

Our present objective is to check the applicability of the TAE method to studying weathering in fossil coal exposed to cyclic freezing and thawing and to estimate the effect of pore water pH on the process.

SAMPLES AND PRECONDITIONING PROCEDURES

We studied dry polished prismatic (30 to 40 mm faces) samples of bituminous (low-caking) and subbituminous (long-flame) hard coals and lignite (Table 1).

Table 1. **Properties of coal samples used in the study**

Coal rank	Mine/coal deposit	Petrography, vol.%				Indicators, wt.%			
		Vt	Sv	I	L	C^{daf}	A^{d}	V^{daf}	S^{d}
Bituminous coal	Bachat/Kuznetsk coal basin	31	24	45	0	85.48	11.3	21.9	0.16
Sub-bituminous coal	Taldin/Kuznetsk coal basin	54	11	27	8	76.39	15.3	38.8	0.37
Lignite	Berezovo/Kansk-Achinsk coal basin	94	–	6	0	56.85	4.3	47.5	0.26

Note: Vt, Sv, I, L = contents of vitrinite, semivitrinite, inertinite, and liptinite, respectively; C^{daf} = content of carbon in dry ash free coal; A^{d} = ash content in dry coal; V^{daf} = contents of volatiles in dry ash free coal; S^{d} = percent of total sulfur per dry weight.

The stability of coal to cracking under temperature changes should depend on the percentages of vitrinite (Vt), as well as carbon and volatiles calculated on the dry ash free basis (C^{daf} and V^{daf}, respectively). Generally, the stability of coal to thermal impacts is inversely proportional to the Vt and V^{daf} contents while coal with lower C^{daf} contains oxygen and is subject to progressive oxidation, with rapid breakdown of bonds in its structure [*Epshtein, 2009; Stolbova and Isaeva, 2013*]. The plots of V^{daf} and C^{daf} vs. Vt (Fig. 1) suggest the highest stability in bituminous coal and the lowest stability in lignite. This information will be used below for checking the results of TAE tests.

Altogether we tested fifty coal samples of each rank. The samples were soaked for 14 days in pH = 5.0 (a half of all samples) and pH = 6.5 solutions (the other half) in order to simulate the effect of acid meteoric waters percolating into coal. The soaked samples reached the maximum water saturation in nine days, according to repeated weighing results. Then the samples of each coal rank were divided into five equal groups and exposed to different numbers of freezing-thawing cycles. The loading consisted of three steps: freezing to –40 °C; exposure to this temperature for 120 min; natural convective thawing to +10 °C. The number of freezing-thawing cycles differed from 3, 6, ... 15 for lignite, sub-bituminous, and bituminous coal samples soaked in pH = 5.0 water to 12, 15, ... 24 for bituminous coal soaked in water with pH = 6.5. Then, the samples were heated to 80 °C at 1.5 °C/min and left for 3 h under this temperature in a tightly sealed cell of the *Nabertherm RT 50/250/11* furnace equipped with a *P 320* digital temperature controller, in order to increase the deformation. The temperature and the exposure time were chosen proceeding from fracture dynamics of coal samples at different temperatures studied using an *OLYMPUS 51BX* microscope. The analysis showed neither formation of new cracks nor growth of oxidized zones in the absence of oxygen inputs at the chosen temperature regime, but the cracks produced by preliminary thermal loading were growing rapidly.

The same inference was obtained from acoustic emission spectra of the heated coal samples (see an example spectrum in Fig. 2). The spectra (Fig. 2) record rapid growth of cracks during slow heating to 80 °C (domain I). The thermal stress of this step is quite low and can break only elastic bonds weakened by cyclic freezing and thawing. Once most of these bonds has broken up, the AE activity ($\dot{N}_{\Sigma}$, pulse/s) decreases to the background level. The activity $\dot{N}_{\Sigma}$ remains within the background during further exposure of the sample to T^{0}_{max} (domain II in Fig. 2), which confirms the ability of coal stable to freeze-thaw weathering to sustain the applied temperature without further growth of cracks and formation of new non-cryogenic defects. Thus, the applied thermal loading regime simulates properly the climate-induced deformation and, on the other hand, speeds it up. Deformation occurs under the following conditions:

– smooth temperature fluctuations, at a minor bulk temperature gradient;

– no rapid moisture release; all chemically bound liquid stays in the samples;

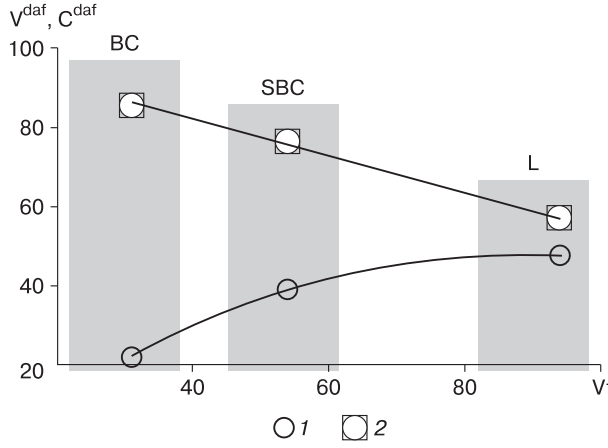

Fig. 1. Contents of volatiles V^{daf} (*1*) and carbon C^{daf} (*2*) in dry ash free coal as a function of vitrinite contents (Vt) in bituminous (BC) and sub-bituminous (SBC) coal and in lignite (L).

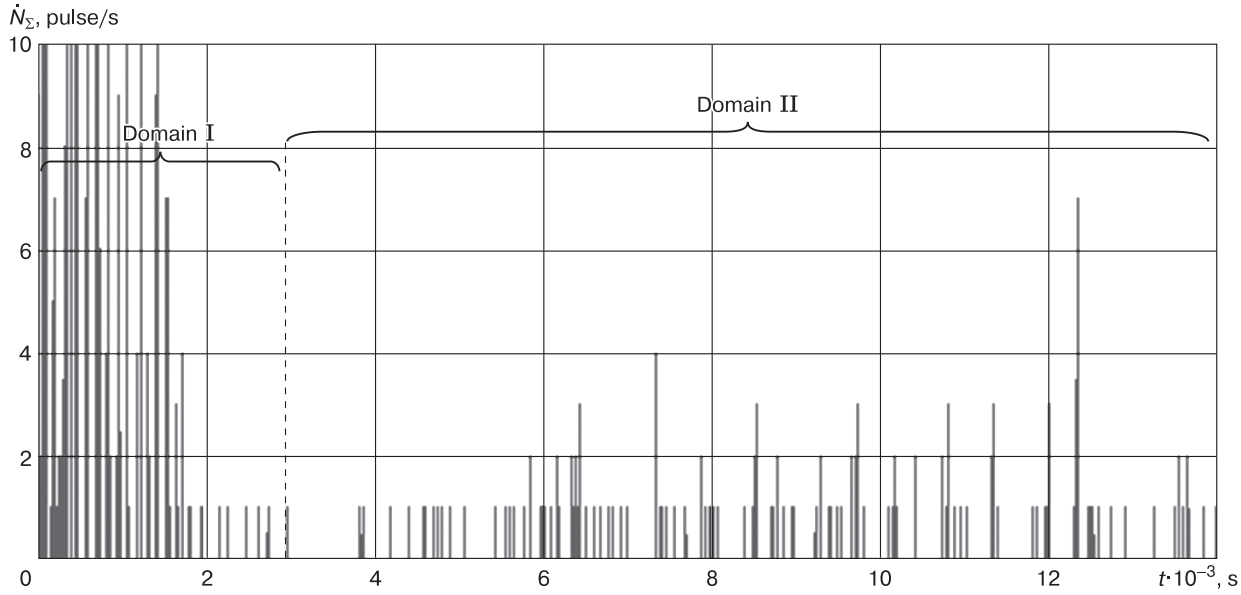

Fig. 2. Activity of acoustic emission $\dot{N}_\Sigma$ as a function of time t after the onset of thermal loading.
Loading protocol: heating from 25 to 80 °C at 1.5 °C/min, exposure to T^0_{max} = 80 °C for 180 min.

– progressive surface oxidation and rapid thermal expansion (at different rates for different elements of coal structure) cause no additional deformation.

These conditions increase the intensity of thermally induced cracking while its style remains the same. The weathering degree of coal samples depends on the number of freezing-thawing cycles.

INSTRUMENTS AND METHODS

During the experiments, the acoustic emission responses of samples to thermal loading were recorded with an *A-Line 32D* system. The samples were exposed to thermal shocks by fast heating to temperatures of 120 to 190 °C at ≈15 °C/min, in two steps: the applied heat flux provided heating to a maximum temperature of T^{I}_{max} = 120–140 °C at the first step and $T^{II}_{max} = T^{I}_{max}$ + (30–50) °C at the second step. The temperature was monitored with an *ATA-2102* thermocouple connected with an *ATE-9380* system, to a precision of ±(0.5 % of the measured value +0.5 °C).

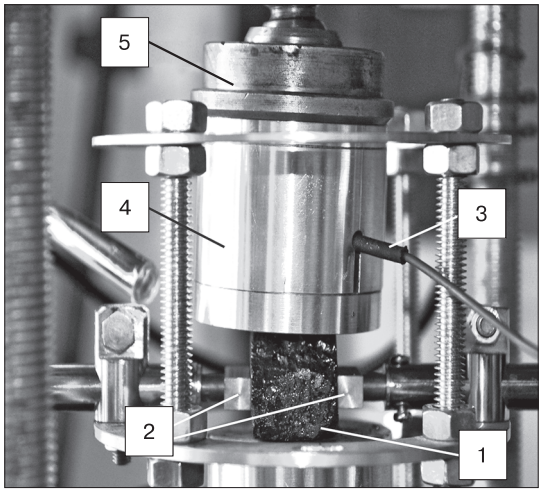

Fig. 3. Laboratory system for thermal loading of coal samples and simultaneous recording of AE parameters (numbers are explained in text).

The thermal loading simulated temperature variations in non-sheltered pre-weathered coal in a local zone of self-heating or non-uniform heating by external sources (e.g., direct sunlight and/or aerating wind). The AE responses of coal to the thermal shocks bear information on its weathering degree and thermal resistance. The high temperature difference commonly leads to spontaneous combustion of cryogenically weathered coal during its storage and transportation.

The thermal loading (Fig. 3) of samples (1) was effectuated by electric heaters (2) mounted at the sample center, with voltage temperature control. The AE responses were recorded by a transducer (3) placed in a metal case (4); the sample-heater contact was provided by a pressure device (5).

Each heating step lasted until the AE activity reduced to the background value meaning that the coal samples had accommodated the thermal stress, i.e., all bonds not sustaining the respective stress level had broken up, which was recorded as AE sources. The heaters were turned off after each heating step,

and the samples were let cool down naturally for at least 30 min. Two steps were required because the first step signals were noisy owing to release of residual pore water under 120–140 °C, and the noise component was hard to discriminate. Thus, the responses of dry coal to heating at the second step were used for analysis.

APPROACHES TO TAE DATA PROCESSING

Typical AE responses to thermal loading (Fig. 4) comprise several domains. The domains TS I and TS II of peak $\dot{N}_\Sigma$ values correspond to accelerated deformation during first and second thermal shocks, respectively. $\dot{N}_\Sigma$ increase in the domains SC I and SC II corresponds to release of thermal stress during self cooling and return of the survived bonds to the initial state. Thus, the AE activity $\mathrm{M}\left(\dot{N}_\Sigma^{\mathrm{TS}}\right)$ averaged over the duration of heating steps records the rate of crack propagation under temperature variations, while the activity $\mathrm{M}\left(\dot{N}_\Sigma^{\mathrm{SC}}\right)$ averaged over the time of cooling measures the preservation of the initial structure. The absolute values $\mathrm{M}\left(\dot{N}_\Sigma^{\mathrm{TS}}\right)$ and $\mathrm{M}\left(\dot{N}_\Sigma^{\mathrm{SC}}\right)$ are inapplicable to comparative measurements because of their random dependence on the size of coal samples, presence of inclusions, bedding direction, etc. Given that these factors affect the AE generation mechanisms during both increasing and decreasing thermal stress, the ratio $k_{\mathrm{td}} = \mathrm{M}\left(\dot{N}_\Sigma^{\mathrm{TS}}\right)/\mathrm{M}\left(\dot{N}_\Sigma^{\mathrm{SC}}\right)$, free from random effects, was used to estimate the properties of coal. Physically, this ratio relates the number of coal structure bonds broken by a thermal shock to that of unbroken bonds, and thus records the stability of coal to thermal-stress weathering. Another informative parameter we used was the duration of AE responses (D_{imp}, 10^{-6} s) corresponding to the time required for the applied stress to cause an elementary deformation event that may induce acoustic emission above the trigger threshold of the measuring system. Only the signals that exceed the threshold can be discriminated from noise.

To avoid effects of random noise present in all AE parameters (see above), D_{imp} was normalized to the dimensionless coefficient $K^{\mathrm{imp}} = D_{\mathrm{imp}}^{\mathrm{TS}} / D_{\mathrm{imp}}^{\mathrm{SC}}$: a ratio of D_{imp} values averaged over the time domains of loading (thermal shock) and unloading (self cooling), respectively. In terms of physics, K^{imp} relates the rate of crack growth under increasing thermal stress to the rate at which the survived bonds return to the initial state after the heating has stopped. K^{imp} most strongly depends on $D_{\mathrm{imp}}^{\mathrm{TS}}$ as the thermal shock affects each individual bond and, if this bond sustains the shock, the time of subsequent relaxation is poorly sensitive to the total number of broken bonds.

The ratio $R^{\mathrm{t}} = k_{\mathrm{td}}/K^{\mathrm{imp}}$, in its turn, accounts for the effect of weathering on both the activity and average duration of AE signals. R^{t} is an acoustic emission measure of the rates of crack growth and coal oxidation as a function of weathering degree.

TAE DATA PROCESSING AND INTERPRETATION

According to the above approach, all calculations were performed for the domains TS II and SC II when the responses are free from residual pore water effects. The testing results are presented in Fig. 5 as the parameter R^{t} plotted against the number of freezing-thawing cycles (S). The points in the $R^{\mathrm{t}}(S)$ curves (Fig. 5) are R^{t} values averaged over at least two replica samples. The plot lacks results for lignite samples

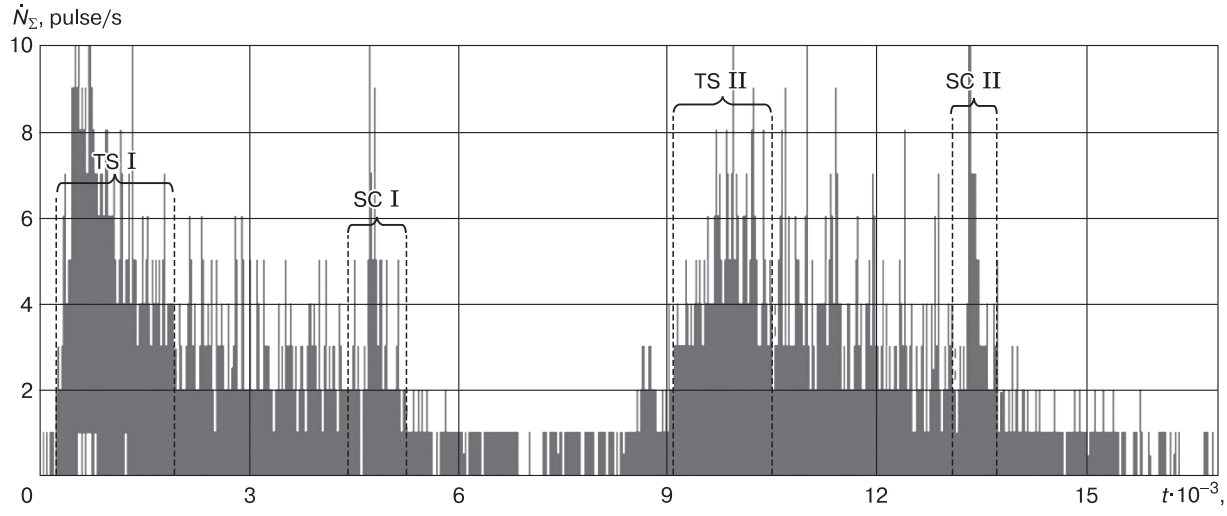

Fig. 4. Typical acoustic emission responses of preliminarily deformed coal to heating (two thermal shocks: $T_{\max}^{\mathrm{I}}$ = 120 °C and $T_{\max}^{\mathrm{II}}$ = 180 °C).

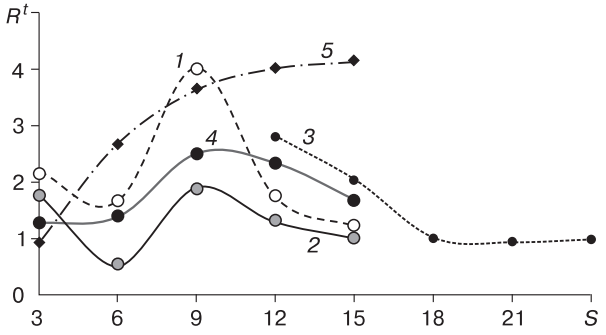

Fig. 5. R^t as a function of the number of freezing-thawing cycles (S) applied to samples of bituminous coal (BC), sub-bituminous coal (SBC), and lignite (L) saturated with waters of pH = 5.0 and 6.5.

1 – sub-bituminous coal, pH = 6.5; *2* – sub-bituminous coal, pH = 5.0; *3* – bituminous coal, pH = 6.5; *4* – bituminous coal, pH = 5.0; *5* – lignite, pH = 5.0.

saturated with pH = 6.5 water because most of them had failed before the tests ended. As follows from Fig. 1 and Table 1, lignite originally had very low thermal resistance and was more vulnerable to weathering.

The photographs (Fig. 6) of samples deformed to different degrees under the test thermal loading demonstrate that the cracks are restricted to the interior of the samples where most of pore moisture resides and coal is undisturbed yet, while a coat of weathered (oxidized) coal forms on the surface. Note that surface fracture prior to the tests was insignificant (not shown in Fig. 6).

The weathering history of the hard coal samples includes several stages (Fig. 5):

Stage I ($S \leqslant 6$): few new defects form; coal strength remains almost invariable; deformation is restricted to growth of the existing cracks; as all these cracks have been involved, the weathering rate decreases, and the function $R^t(S)$ decays correspondingly.

Stage II ($6 < S \leqslant 12–18$, depending on coal rank): most rapid growth of the existing cracks which serve as air guides. As a result, coal becomes progressively more oxidized (at an avalanche rate) and less stable. As the strength reaches the threshold value, new defects form rapidly and the network of connected cracks covers ever greater volume. The oxygenated gas mixture replaces the originally inert pore gas, which maintains the most rapid weathering shown up as a peak of the $R^t(S)$ function.

Stage III ($S > 12–18$): accumulation of defects continues but the cracking rate decays as the number of undeformed sites in the samples tends to zero (flattening of the $R^t(S)$ curve).

Visual examination of samples after thermal loading confirms that the weathering process is multistage. A visible network of cracks at stage I (Fig. 6, *a*) forms only at the immediate contact of coal with the heaters. At stage II, some coal samples experience sintering (Fig. 6, *b*), which may lead to spontaneous combustion in natural conditions (e.g., at strong wind). Weathering of coal under cyclic thermal stress at stage III eventually leads to its disintegration (Fig. 6, *c*) but no sintering occurs. Therefore, coal undergoes over-oxidation, and its calorific value decreases to the degree when ignition requires a high external heat flux and special conditions.

The $R^t(S)$ pattern for lignite differs markedly from that of the hard coal samples: the weathering rate begins increasing already since the lowest freezing temperature and then grows exponentially. In other words, the state of lignite at any notable freeze-thaw effect always corresponds to stage II. This is another piece of evidence that lignite is originally weak and can develop new defects since the first freezing-thawing cycle (i.e., it skips stage I). The lignite samples have zero residual thermal resistance and never reach stage III. At the deformation threshold, lignite becomes disintegrated and(or) oxidized while hard coal preserves some structural integrity and fails only at $S > 12–18$ (see $R^t(S)$ in Fig. 5).

Note that coal of the same rank degrades more slowly (smaller $R^t(S)$ peaks) when saturated with more acid water. The reason may be in various interaction mechanisms of coal and acid solutions which require separate consideration. One possible mechanism is as follows. The effect of acid solutions on coal can be considered as hydrolysis whereby non-aromatic bridge atoms between aromatic lamelli in the organic coal component react with dissolved acids [*Saranchuk et al., 1988*]. Since coal is hydrophobic, this interaction occurs on the sample surfaces and on the walls of open cracks which channel solutions percolating inward the coal samples. The thermal shock stimulates additionally the reactions on the sample surface and on the crack walls. The reactions remove residual water, as well as carbon oxides produced by breakdown of non-aromatic bridges and adsorbed gases.

In addition to cracking, the general reactivity of coal decreases. Thus, the contact of coal with a low-pH medium leads to surface deformation and, on the other hand, to better ordering of the coal structure. Either deformation or structure change may predominate depending on the coal rank and water pH: the lower the pH, the stronger the primary effect on coal and the more prominent the structure formation. The latter process has multiple controls and increases the energy of bonding between aromatic lamelli, which may impede crack propagation.

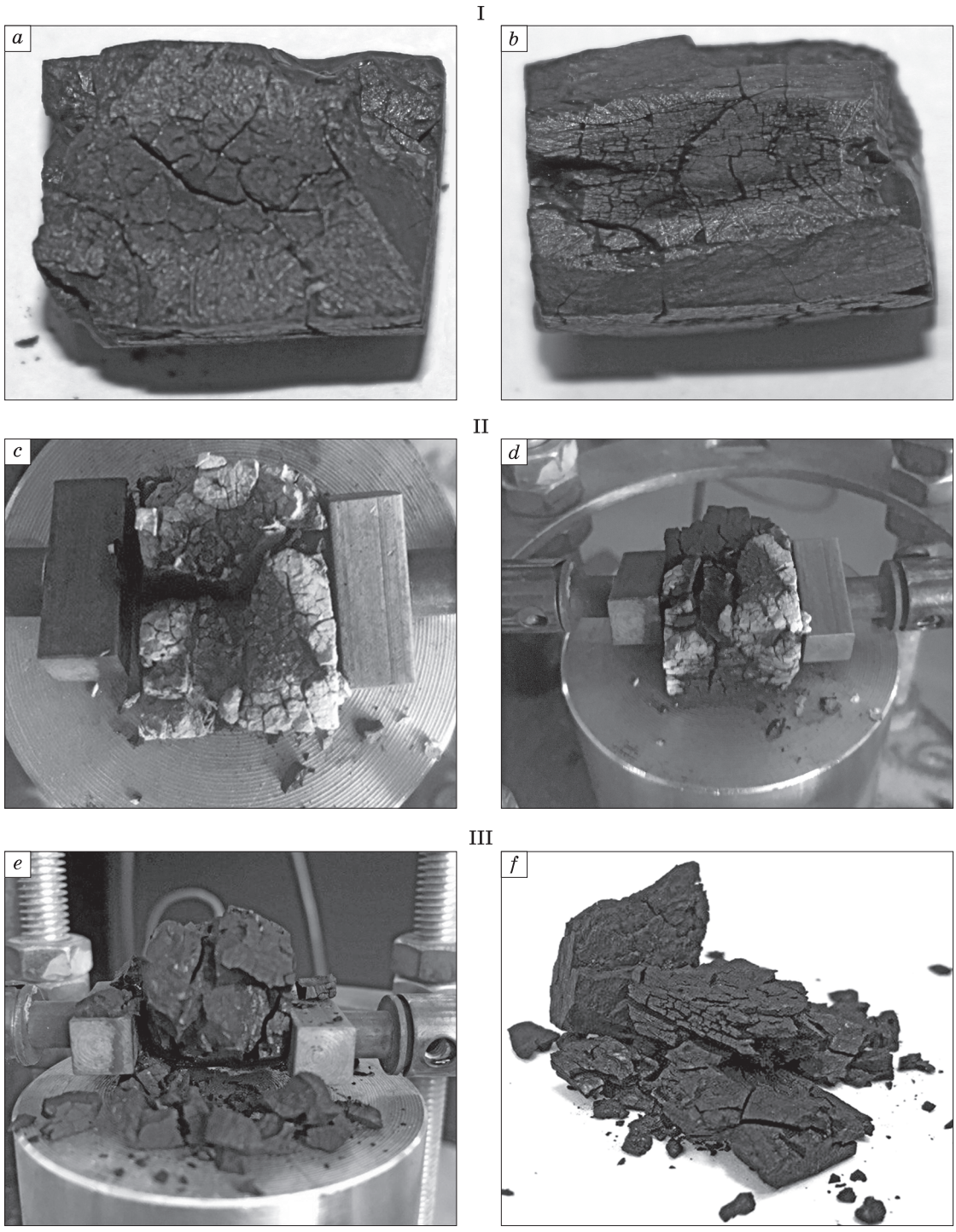

Fig. 6. Typical view of the tested coal samples at weathering stages I–III, two photographs for each stage: *a*, *b* (stage I); *c*, *d* (stage II); *e*, *f* (stage III).

Note also that the reactions of coal with acid solutions lead to leaching of salts which fill cracks with saline water. As water evaporates, salts precipitate on the crack walls and form a coat that prevents coal from contact with air and thus reduces the rate of oxidation and weathering. Furthermore, the lower freezing temperature of saline water compared to fresh water may decelerate the formation of pore ice that wedges the cracks out during freezing-thawing cycles.

CONCLUSIONS

The reported testing was applied to a representative number of hard coal and lignite samples exposed to cyclic freezing and thawing that simulates weathering in cold regions. The activity and duration of the acoustic emission responses of samples to thermal loading correlate with the rate of weathering depending on pH of water saturating the coal. The suggested TAE method can track the history of coal weathering by periglacial processes.

The freeze-thaw weathering of coal can be characterized with several parameters. They are, specifically, the ratio (R^t) that measures the oxidation rate of coal related with its cracking. The deformation degree, in its turn, is inferred from the number of freezing-thawing cycles (S) applied to the samples. As proven by the tests, the ratio R^t is applicable to estimate the rate of weathering in fossil coal and to predict the related deterioration of its technological properties. The function R^t has a rising segment, depending on the degree of deformation, which corresponds to low calorific value and extremely rapid oxidation of coal leading to spontaneous combustion. Before the rise of $R^t(S)$, the effect of freezing and thawing is minor and fails to induce the formation of new cracks. At this stage, there are no prerequisites for aeration and the ensuing rapid oxidation fraught with spontaneous heat generation. The end of the peak segment and $R^t(S)$ flattening correspond to the decay of the weathering process and deceleration of oxygen migration as the number of non-oxidized sites in coal tends to zero. For the same reason, ignition of over-oxidized coal is hardly probable without external heating.

The effect of relatively acid solutions (pH = = 5.0–6.5) on coal exposed to cyclic freezing and thawing reduces the rate of its weathering and may be due to various mechanisms, which require further investigation. One possible mechanism may be that coal becomes generally less reactive upon contact with a low-pH medium while the increasing energy of bonds between aromatic lamelli impedes crack propagation. Another possibility is that acid solutions leach salts from coal, whereby cracks become filled with saline water and salt precipitates on the crack walls as the water evaporates; the salt coats impede the aeration of coal and thus reduce oxidation and decelerate weathering.

The suggested approaches allow express testing of the coal state in the field. By repeated sampling and testing, one can monitor time-dependent changes in the parameter R^t and compare the results with those for recently extracted samples. Rapid R^t increase in coal of the same rank indicates that the samples have reached the stage of low calorific capacity and high risks of oxidation and spontaneous combustion.

The study was supported by grant 16-05-00033 A from the Russian Foundation for Basic Research.

References

ASTM D5263-15, 2015. Standard test method for determining the relative degree of oxidation in bituminous coal by alkali extraction. Gaseous Fuels. Coal and Coke 05.06, 3.

Epshtein, S.A., 2009. Mechanic properties of vitrinite in coal of different grades. Gorn. Inform.-Analit. Bul., No. 8, 58–69.

Fedorova, S.E., 2009. Problems of fire and environment safety in coal mining in permafrost. Gorn. Inform.-Analit. Bul., No. 12, 329–333.

Gresov, A.I., Obzhirov, A.I., Yatsuk, A.V., 2014. Geostructural regularities of the distributions of permafrost in gas- and coal-bearing basins in the North-East of Russia. Kriosfera Zemli XVIII (1), 3–11.

Jun Deng, Yang Xiao, Qingwei Li, Junhui Lu, Hu Wen., 2015. Experimental studies of spontaneous combustion and anaerobic cooling of coal. Fuel 157, 261–269.

Novikov, E.A., Shkuratnik, V.L., Epshtein, S.A., Nesterova, V.G., Dobryakova, N.N., 2013. Possibility for estimating the oxidation state of coal from acoustic emission stimulated by thermal shocks. Gorn. Inform.-Analit. Bul., No. 8, 90–96.

Qian Zhu, 2014. Coal Sampling and Analysis Standards (Analytical Review). IEACCC Ref: CCC/235, IEA Clean Coal Centre, April, 123 pp.

Raja, S., Srivastava, S.K., Singh, M.M., 2009. Aerial oxidation of coal-analytical methods, instrumental techniques and test methods: A survey. Indian J. Chem. Technol. 16, 103–135.

Rogov, V.V., 2009. Fundamentals of Cryogenesis. Geo Publishers, Novosibirsk, 203 pp. (in Russian)

Saranchuk, V.I., Airuni, A.T., Kovalev, K.E., 1988. Supramolecular Structure and Properties of Coal. Naukova Dumka, Kiev, 190 pp. (in Russian)

Shi-Qi, Liu, Shu-Xun, Sang, Hui-Hu, Liu, Qi-Peng, Zhu, 2015. Growth characteristics and genetic types of pores and fractures in a high-rank coal reservoir of the southern Qinshui basin. Ore Geology Rev. 64, 140–151.

Shkuratnik, V.L., Novikov, E.A., 2017. Thermally stimulated emission in rocks as a promising monitoring tool. Gornyi Zhurnal, No. 6, 21–27.

Shkuratnik, V.L., Novikov, E.A., Voznesenskiy, A.S., Vinnikov, V.A., 2015. Thermally Stimulated Acoustic Emission in Rocks. Gornaya Kniga, Moscow, 241 pp. (in Russian)

Stolbova, N.F., Isaeva, E.R., 2013. Petrlogy of Coal. Tomsk Polytechnical University, Tomsk, 77 pp. (in Russian)

Timofeev, A.A., Cherepovskiy, V.F. (Eds.), 2000–2003. Coal Resources of Russia. Books 1–4. Coal Basins and Deposits of Russia. Geoinformmark, Moscow, 2068 pp. (in Russian)

Verkhoturov, A.G., Razmakhnina, I.B., 2016. Causes of deformation in the sides of open coal mines in Transbaikalia. Gorn. Inform.-Analit. Bul., No. 9, 211–221.

Yanmei, Yu, Weiguo, Liang, Yaoqing, Hu, Qiaorong, Meng., 2012. Study of micro-pores development in lean coal with temperature. Intern. J. Rock Mechanics and Mining Sci. 51, 91–96.

Yershov, E.D., 2002. General Geocryology. Moscow University Press, Moscow, 682 pp. (in Russian)

Received October 19, 2017